



Robust Output Feedback Stabilization and Boundedness of Highly Nonlinear Induction Motors Systems Using Single-Hidden-Layer Neural-Networks

H. Ait Abbas^{1*}, A. Seghiorou², M. Belkheiri³ and M. Rahmani³

¹ *Laboratory of Materials and Durable Development-LM2D, Electrical Engineering Department, Faculty of Sciences and Applied Sciences, University of Bouira, (10000) Bouira, Algeria.*

² *Electrical Engineering Department, Higher School of Electrical Engineering and Energetic, (31000) Oran, Algeria.*

³ *Laboratory of Telecommunications Signals and Systems, Amar Telidji University – Laghouat, BP G37 Road of Ghardaia (03000 Laghouat), Algeria.*

Received: December 2, 2018; Revised: June 13, 2019

Abstract: This paper presents a new single-hidden-layer neural-network (SHL NN)-based adaptive input-output feedback linearization control (IOFLC) to handle the flux and speed tracking problems of the induction motor (IM) subjected to unknown parametric uncertainty, modelling errors and external load disturbances. In this approach, we first apply the IOFLC to divide the IM dynamics into two decoupled subsystems. The resulted controller is then augmented via an on-line SHL NN in order to overcome effects of both the neglected dynamics and the modeling errors. The NN is lunched over input-output signals of the controlled system. The adaptive laws augmented using NN parameters are expressed in terms of the estimated tracking error dynamics of the nominal systems. Of main interest, Lyapunov's direct method is involved to exhibit the ultimate boundedness of the error signals. Computer simulations are presented to emphasize the practical potential of the proposed approach.

Keywords: *nonlinear systems; feedback control; perturbations; adaptive or robust stabilization; neural nets and related approaches; stability; boundedness; simulation.*

Mathematics Subject Classification (2010): 93C10, 93B52, 93C73, 93D21, 62M45, 70K20, 34C11, 37M05.

* Corresponding author: <mailto:h.aitabbas@univ-bouira.dz>

1 Introduction

The IMs are widely used as electromechanical actuators due to their being rugged, free of maintenance, low cost and generally less expensive than other electrical machines [2, 5]. These motors have been utilized for more and more extensive industrial applications such as electric railways and robots, where advanced dynamic performance is claimed. However, the IM considered as a multivariable system has such characteristics as high-coupling and high nonlinearity, which implies that it is very difficult to control.

In the past two decades, trajectory tracking control of the IM systems has been amply studied due to the exigency of high performance in the context of excellent tracking accuracy, rejection of both structured (external disturbances) and unstructured uncertainties (parameter variations and unmodelled dynamics) [2]. For that purpose, the field-oriented control (FOC) scheme will be applied for the IM nonlinear system so as to achieve similar performance characteristics of a separately excited DC motor, such fast, precise tracking, which makes the control task easy [5]. However, some drawbacks such as the coupling between speed and flux and unmodelled dynamics subjugate thoughtful constraints for the FOC and effect the performance speed tracking accuracy. Further, since unknown parametric uncertainties often exist in IM dynamics and they are source of instability, it is meaningful to consider control problems of the corresponding nonlinear IM model [2, 5].

Nowadays, practical issues narrow down the choice and give a significant advantage to the input-output feedback linearization control (IOFLC) that is among the most powerful techniques to perform an exact decoupling between both speed and flux dynamics, and higher power efficiency [12]. Furthermore, with the developments of nonlinear control theory and methods (sliding-mode control [14, 18], backstepping approach [7, 16], and nonlinear feedback linearization control [5, 8, 17]), the control of IMs subjected to uncertainties has become an important research topic. Specifically, substantial attention has been focused on the use of SHL NN in the system modelling and control applications due to their advantageous features including high potential to identify nonlinear behaviors, powerful nonlinear mapping between inputs and outputs without faithful knowledge of the system model [20].

Moreover, the adaptive control results motivate researchers to find new structures that do not rely on completely knowing the system nonlinearities by using approximation property of NNs and fuzzy logic approximators [4, 9, 19]. The author in [13] presents a new adaptive controller which rules out the effect of uncertainties in order to achieve precise position-tracking performance of IMs using a radial basis function neural network (RBF NN). In [6], the authors develop a new adaptive backstepping controller of a nonlinear IM that achieves global asymptotic speed tracking for the full-order, despite the uncertainty in rotor resistance and external disturbance (load torque). The work presented in [16] deals the tracking control problem of IMs subject to disturbances in practical applications, in which both fuzzy logic control scheme is involved to identify the term of nonlinearities and an adaptive backstepping method is employed to elaborate an adaptive term that eliminates these nonlinearities. An adaptive fuzzy vector controller (AFVC) is established in the paper [10] to cover the speed and torque tracking problem of a doubly-fed IM, in which the control conception is carried thanks to an appropriate backstepping method that ensures inherently the stability of the control system.

Motivated by the aforesaid discussion, we propose to combine SHL NNs that show strong potentials in approximating uncertainties, with the IOFLC methodology in order to originate a variety of control schemes within the context of NN-based adaptive input-

output feedback control, which can be extended for an extensive class of nonlinear systems with unmodeled dynamics. The elaborated controller takes on dynamic compensator to stabilize the linearized system. Note that the vector that contains the measured tracking error and compensator states is exploited to adapt the NN weights. The input vector to the NN is composed of input/output data, and the adaptive terms adjust on-line for high nonlinearities using nonlinearly parameterized SHL NN. The stability analysis is presented in order to both build the NN adaptation law using only unappropriated measurement as a training signal, and reveal boundedness of all the error signals of the controlled system.

The rest of the paper is organized as follows. The IM model and problem statement are presented in Section 2. Section 3 contains the FOC and IOFLC NN augmentation and the design control for the IM are detailed in Section 4. Section 5 describes the SHL NN implementation. The stability analysis is detailed in Section 6. The effectiveness of the proposed IM control system is demonstrated through simulation results in Section 7.

2 Induction Motor Modeling and Problem Statement

2.1 Mathematical model of the IM

The IM is represented by the model [12]

$$\begin{cases} \frac{dw}{dt} = \frac{n_p L_m}{J L_r} (i_{sb} \psi_{ra} - i_{sa} \psi_{rb}) - \frac{f}{J} w - \frac{\tau_L}{J}, \\ \frac{d\psi_{ra}}{dt} = -\frac{R_r}{L_r} \psi_{ra} - n_p w \psi_{rb} + \frac{R_r}{L_r} L_m i_{sa}, \\ \frac{d\psi_{rb}}{dt} = n_p w \psi_{ra} - \frac{R_r}{L_r} \psi_{rb} + \frac{R_r}{L_r} L_m i_{sb}, \\ \frac{di_{sa}}{dt} = \frac{L_m R_r}{\sigma L_s L_r^2} \psi_{ra} + \frac{n_p L_m}{\sigma L_s L_r} w \psi_{rb} - \left(\frac{L_m^2 R_r + L_r^2 R_s}{\sigma L_s L_r^2} \right) i_{sa} + \frac{1}{\sigma L_s} u_{sa}, \\ \frac{di_{sb}}{dt} = -\frac{n_p L_m}{\sigma L_s L_r} w \psi_{ra} + \frac{L_m R_r}{\sigma L_s L_r^2} \psi_{rb} - \left(\frac{L_m^2 R_r + L_r^2 R_s}{\sigma L_s L_r^2} \right) i_{sb} + \frac{1}{\sigma L_s} u_{sb}. \end{cases} \quad (1)$$

Notice that i, ψ, u_s denote current, flux linkage and stator voltage input to the machine. The variable w denotes the speed of the rotor, while θ is the rotor position. L_r, L_s , and L_m denote the rotor, stator, and mutual inductances, R_r and R_s are the rotor and stator resistances, J is the rotor’s moment of inertia, f denotes the coefficient of viscous friction, τ_L is the load torque, and n_p is the number of pole pairs; the subscripts “s” and “r” stand for the stator and rotor; (a, b) represent vector components with respect to a fixed stator reference frame in which $\sigma = 1 - L_m^2 / (L_s L_r)$. From now on we will skip the subscripts “r” and “s” since we will only utilize the state variables of rotor fluxes (ψ_{ra}, ψ_{rb}) and stator currents (i_{sa}, i_{sb}) .

Let $x = (w, \psi_a, \psi_b, i_a, i_b)^T$ be the state vector, and

$$p = (\delta_1, \delta_2, \delta_3)^T = (\tau_L - \tau_{LN}, R_r - R_{rN}, R_s - R_{sN})^T \quad (2)$$

be the unknown parameter deviations from the nominal values τ_{LN}, R_{rN} and R_{sN} of the load torque τ_L , rotor resistance R_r and stator resistance R_s . However, τ_L is typically unknown, whereas R_r and R_s may have a range of variations of $\pm 100\%$ around their nominal values due to ohmic heating. Let $u = (u_a, u_b)^T$ be the control vector. Let $\alpha =$

R_{rN}/L_r , $\beta = L_m/(\sigma L_s L_r)$, $\gamma = (L_m^2 R_{rN}/\sigma L_s L_r^2) + (R_{sN}/\sigma L_s)$, $\mu = n_p L_m/(J L_r)$, $G = (\sigma L_s)$, be a reparameterization of the IM model, where $\alpha, \beta, \gamma, \mu, G$ are known parameters depending on the nominal values R_{rN} and R_{sN} . System (1) can be reformulated in compact form as

$$\dot{x} = f(x) + u_a g_a + u_b g_b + \delta_1 f_1(x) + \delta_2 f_2(x) + \delta_3 f_3(x), \quad (3)$$

where the vector fields $f, g_a, g_b, f_1, f_2, f_3$ are

$$f(x) = \begin{pmatrix} \mu(i_b \psi_a - i_a \psi_b) - \frac{f}{J} w - \frac{\tau_{LN}}{J}, \\ -\alpha \psi_a - n_p w \psi_b + \alpha L_m i_a, \\ n_p w \psi_a - \alpha \psi_b + \alpha L_m i_b, \\ \alpha \beta \psi_a + n_p \beta w \psi_b - \gamma i_a, \\ -n_p \beta w \psi_a + \alpha \beta \psi_b - \gamma i_b. \end{pmatrix}, \quad f_1(x) = \begin{pmatrix} -\frac{1}{J} \\ 0 \\ 0 \\ 0 \\ 0 \end{pmatrix},$$

$$f_2(x) = \begin{pmatrix} 0 \\ -\frac{1}{L_r} \psi_a + \frac{L_m}{L_r} i_a \\ -\frac{1}{L_r} \psi_b + \frac{L_m}{L_r} i_b \\ \frac{L_m}{\sigma L_s L_r^2} \psi_a - \frac{L_m^2}{\sigma L_s L_r^2} i_a \\ \frac{L_m}{\sigma L_s L_r^2} \psi_b - \frac{L_m^2}{\sigma L_s L_r^2} i_b \end{pmatrix}, \quad f_3(x) = \begin{pmatrix} 0 \\ 0 \\ 0 \\ -\frac{1}{G} \\ -\frac{1}{G} \end{pmatrix}, \quad g_a = \begin{pmatrix} 0 \\ 0 \\ 0 \\ \frac{1}{G} \\ 0 \end{pmatrix}, \quad g_b = \begin{pmatrix} 0 \\ 0 \\ 0 \\ 0 \\ \frac{1}{G} \end{pmatrix}.$$

2.2 Control problem statement

This paper focuses on the study of tracking control ($(w \rightarrow w^*)$ and $(\psi_d = \sqrt{\psi_{ra}^2 + \psi_{rb}^2} \rightarrow \psi_d^*)$) for the field-oriented IM subject to external disturbances (load torque) and parameter uncertainties. For that matter, we contribute to develop an adaptive input-output feedback linearization technique to elaborate controllers in which SHL NNs are used to approximate terms of nonlinearity.

3 Field-Oriented and Input Output Linearization Control

3.1 Conventional field-oriented control

The control objective is to conceive a controller in which the stator voltages are chosen to adjust the torque, speed and/or position of the motor. To achieve the field-oriented control, we perform the transformation of the vectors (i_a, i_b) and (ψ_a, ψ_b) in the fixed stator frame (a, b) into vectors in a frame (d, q) which rotate along with the flux vector $((\psi_a, \psi_b))$. Therefore, the stator phase currents and voltages are then expressed in this new coordinates as follows [7]

$$\begin{bmatrix} i_d \\ i_q \end{bmatrix} = \begin{bmatrix} \cos \rho & \sin \rho \\ -\sin \rho & \cos \rho \end{bmatrix} \begin{bmatrix} i_{sa} \\ i_{sb} \end{bmatrix}, \quad \begin{bmatrix} u_d \\ u_q \end{bmatrix} = \begin{bmatrix} \cos \rho & \sin \rho \\ -\sin \rho & \cos \rho \end{bmatrix} \begin{bmatrix} u_{sa} \\ u_{sb} \end{bmatrix}$$

in which we define $(\rho = \arctan(\frac{\psi_b}{\psi_a}))$, where ψ_d and ρ are just "polar coordinates" for the ordered pair (ψ_a, ψ_b) . The term "field-oriented" affects this new rotating coordinate

system in which the angular position is ρ so that $\psi_q \equiv 0$, and i_d and i_q are called the direct and quadrature currents, u_d and u_q are called the direct and quadrature voltages, respectively.

When we refer to the fixed stator (d, q) reference frame, the electromagnetic dynamic model of the induction motor can be developed yielding

$$\begin{cases} \frac{dw}{dt} = \mu\psi_d i_q - \frac{f}{J}w - \frac{\tau_L}{J}, \\ \frac{d\psi_d}{dt} = -\alpha\psi_d + \alpha L_m i_d, \\ \frac{di_d}{dt} = -\gamma i_d + \alpha\beta\psi_d + n_p w i_q + \alpha L_m \frac{i_q^2}{\psi_d} + \frac{1}{G}u_d, \\ \frac{di_q}{dt} = -\gamma i_q - \beta n_p w \psi_d - n_p w i_d - \alpha L_m \frac{i_d i_q}{\psi_d} + \frac{1}{G}u_q, \\ \frac{d\rho}{dt} = n_p w + \alpha L_m \frac{i_q}{\psi_d}. \end{cases} \tag{4}$$

Now, it is clear that the electromagnetic torque $\tau_e = J\mu\psi_d i_q$ is just proportional to the product of two state variables ψ_d and i_q . Unfortunately, in the state space model of the IM presented in (4), differential equations for i_d and i_q nevertheless include plenty high nonlinearities. For that, one possibility to make simpler these dynamics is to involve the nonlinear state feedback control

$$\begin{bmatrix} u_d \\ u_q \end{bmatrix} = G \begin{bmatrix} \gamma i_d - \alpha\beta\psi_d - n_p w i_q - \alpha L_m \frac{i_q^2}{\psi_d} + \bar{v}_d \\ \gamma i_q + \beta n_p w \psi_d + n_p w i_d + \alpha L_m \frac{i_d i_q}{\psi_d} + \bar{v}_q \end{bmatrix}. \tag{5}$$

Then, the resulting closed-loop IM system is written as

$$\begin{cases} \frac{dw}{dt} = \mu\psi_d i_q - \frac{f}{J}w - \frac{\tau_L}{J}, \\ \frac{di_q}{dt} = \bar{v}_q, \\ \frac{d\psi_d}{dt} = -\alpha\psi_d + \alpha L_m i_d, \\ \frac{di_d}{dt} = \bar{v}_d, \\ \frac{d\rho}{dt} = n_p w + \alpha L_m \frac{i_q}{\psi_d}, \end{cases} \tag{6}$$

where $\psi_d(t)$ and $w(t)$ are output signals of the IM that will be controlled to achieve the tracking accuracy.

3.2 Input-output linearization control

In the above FOC scheme, the speed w and flux ψ_d are only asymptotically decoupled. Consequently, the speed is linearly related to i_q only after ψ_d is constant. However, field weakening (i.e., decreasing ψ_d) is necessary for high speeds so as not to saturate the stator voltages. Since field-weakening depends on speed, the dynamics of ψ_d may interfere with the dynamics of w , especially when the speed varies rapidly [12].

As a solution to the presented problem, we suggest to introduce an input-output linearization controller that will be designed for the full order (voltage command) system model (6). Specifically, the transformation ($\eta = \mu\psi_d i_q$, $\psi_d = \psi_d$, $\xi = -\alpha\psi_d + \alpha L_m i_d$) is introduced for (6), resulting in

$$\begin{cases} \frac{dw}{dt} = \eta - \frac{f}{J}w - \frac{\tau_L}{J}, \\ \frac{d\eta}{dt} = \mu\xi i_q + (\mu\psi_d)\bar{v}_q, \\ \frac{d\psi_d}{dt} = \xi, \\ \frac{d\xi}{dt} = -\alpha\xi + (\alpha L_m)\bar{v}_d, \\ \frac{d\rho}{dt} = n_p w + \alpha L_m \frac{\eta}{\mu\psi_d^2}, \end{cases} \quad (7)$$

in which v_d and v_q are two new inputs, the application of the feedback

$$\begin{cases} \bar{v}_d = \frac{\xi}{L_m} + \frac{v_d}{\alpha L_m}, \\ \bar{v}_q = -\frac{\mu\xi i_q}{\mu\psi_d} + \frac{v_q}{\mu\psi_d} \end{cases} \quad (8)$$

results in the input-output linearized system

$$\begin{cases} \frac{dw}{dt} = \eta - \frac{f}{J}w - \frac{\tau_L}{J}, \\ \frac{d\eta}{dt} = v_q + \delta_q, \\ \frac{d\psi_d}{dt} = \xi, \\ \frac{d\xi}{dt} = v_d + \delta_d, \\ \frac{d\rho}{dt} = n_p w + \alpha L_m \frac{\mu\eta}{\psi_d^2}, \end{cases} \quad (9)$$

where both δ_d and δ_q denote inversion errors. To explain, assuming that all parametric uncertainties terms for each subsystem are an error signal δ_i (δ_d and δ_q), we take into account the motor parameters R_r and R_s that can vary appreciably due to the Ohmic heating while the magnetic saturation can cause variations of L_r and L_s [6].

It is clear that the system (9) is linear from the inputs v_d , v_q to the outputs w , ψ_d . Consequently, the IM dynamics has a straightforward structure since the conceived controller is the *input-output* linearization controller. However, since the designed controller relies completely on the exact values of the IM parameters with total knowledge of the model, the robustness to parametric uncertainty cannot be ensured. Much work in the literature on robust control have been consecrated to handle such problems. The authors in [8, 15] developed an adaptive output feedback controller augmented via a SHL NN for highly complex nonlinear systems to eliminate the effect of unknown variations in plant parameters and structure that can be unknown but bounded, and provided the stability analysis of the closed loop system using the Lyapunov method.

In the present paper, taking the advantage that the flux dynamics is decoupled from the speed dynamics after IOFLC, and inspired by the control ideas in [8,15] that exploit SHL NNs for their approximation ability, we aim to develop a control law that augments the IOFLC scheme by only SHL NNs to sensibly approximate the uncertainties existing in the IM.

4 Adaptive Controller Design

4.1 Control design

Taking advantage from the fact that the IM dynamics (9) is divided into two linear subsystems, we contribute to synthesize adaptive control laws augmented via NN that utilize the available measurements (ψ_d and w) so that the outputs ($\psi_d(t)$ and $w(t)$) track smooth bounded reference trajectories ($\psi_d^*(t)$ and w^*), respectively, with bounded error. That is, the first four equations of (9) may be written as two decoupled linear subsystems, flux dynamics

$$\begin{cases} \frac{d\psi_d}{dt} = \xi, \\ \frac{d\xi}{dt} = v_d + \delta_d \end{cases} \quad (10)$$

and speed dynamics

$$\begin{cases} \frac{dw}{dt} = \eta - \frac{f}{J}w - \frac{\tau_L}{J}, \\ \frac{d\eta}{dt} = v_q + \delta_q, \end{cases} \quad (11)$$

where v_d and v_q are the inputs chosen to force the linear systems (10) and (11) to track a given reference trajectories ψ_d^* and $w^*(t)$, respectively.

Note that both flux and speed subsystems are partially known, and their outputs ψ_d and w have relative degrees equal to 2. Therefore, the output dynamics ($y_d = \psi_d$) and ($y_q = w$) given by (10) and (11), respectively, will be reformulated as

$$\begin{cases} y_d^{(2)} = \ddot{\psi}_d = v_d + \delta_d, \\ y_q^{(2)} = \ddot{w} = v_q + \delta_q, \end{cases} \quad (12)$$

on suggest exploit SHL NNs for their efficiency and ease of implementation in order to deal with the effect of uncertainties (δ). Therefore, the control strategy will be improved by adding adaptive neural network components u_{ad} , u_{aq} in the expressions of the control laws v_d , v_q in order to identify nonlinearities δ_d and δ_q , respectively. The global block diagram of the designed control scheme is illustrated in Figure (1).

Consequently, the pseudocontrols v_d and v_q are chosen to have the form

$$\begin{cases} v_d = \ddot{\psi}_d^* + D_{cd} - u_{ad}, \\ v_q = \ddot{w}^* + D_{cq} - u_{aq}, \end{cases} \quad (13)$$

where $y_c^{(r)} = (\ddot{\psi}_d^*, \ddot{w}^*)$ are the second derivatives ($r = 2$) of the input signals generated by the stable command filters, D_{cd} and D_{cq} denote outputs of the linear dynamic compensators, u_{ad} and u_{aq} represent the adaptive control signals designed to overcome δ_d and δ_q , respectively.

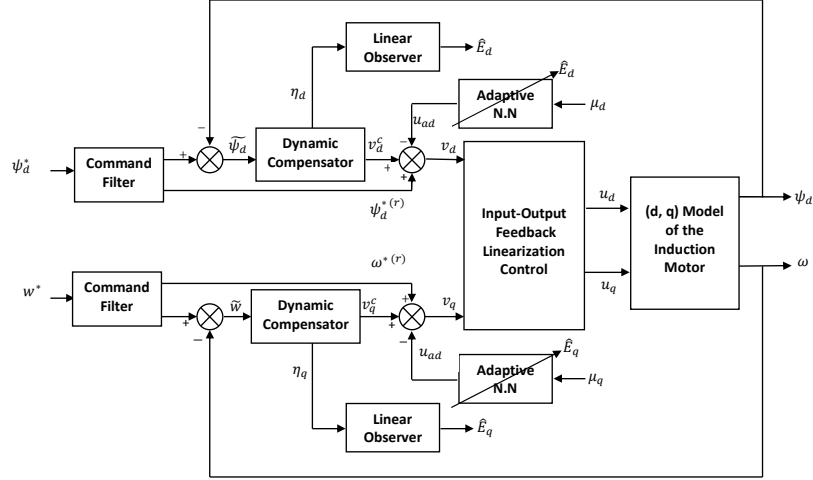


Figure 1: Adaptive input-output feedback linearization controller-based SHL NN architecture.

With (13), the dynamics in (12) reduce to

$$\begin{cases} y_d^{(2)} = \ddot{\psi}_d = \ddot{\psi}_d^* + D_{cd} - u_{ad} + \delta_d, \\ y_q^{(2)} = \ddot{w} = \ddot{w}^* + D_{cq} - u_{aq} + \delta_q. \end{cases} \quad (14)$$

Accordingly, one challenge is to design adaptive input-output feedback linearization controllers, whose adaptive terms u_{ad} and u_{aq} adjust on-line for unknown nonlinearities δ_d and δ_q using nonlinearly parameterized SHL NNs for the flux and speed subsystems, respectively.

Consequently, with (14), the two subsystems (10) and (11) can be rewritten, respectively, as in (15) and (16)

$$\begin{cases} \frac{d\psi_d}{dt} = \xi, \\ \frac{d\xi}{dt} = \ddot{\psi}_d^* + D_{cd} - u_{ad} + \delta_d, \end{cases} \quad (15)$$

$$\begin{cases} \frac{dw}{dt} = \eta - \frac{f}{J}w - \frac{\tau_L}{J}, \\ \frac{d\eta}{dt} = \ddot{w}^* + D_{cq} - u_{aq} + \delta_q. \end{cases} \quad (16)$$

The two subsystems are almost identical, for the rest of the paper we will treat only the dynamics of the flux subsystem to simplify writing

$$\begin{cases} \frac{d\psi_d}{dt} = \xi, \\ \frac{d\xi}{dt} = \ddot{\psi}_d^* + D_{cd} - u_{ad} + \delta_d. \end{cases} \quad (17)$$

4.2 Design of the dynamic compensator and error dynamics

The output tracking errors is defined as $(\tilde{\psi}_d = \psi_d^* - \psi_d)$. Then the dynamics in (14) can be rewritten as

$$\ddot{\tilde{\psi}}_d = -D_{cd} + u_{ad} - \delta_d. \tag{18}$$

The following linear compensator is introduced to stabilize the dynamics in the ideal case ($\delta_d = 0, u_{ad} = 0$)

$$\begin{cases} \dot{\eta}_d = \alpha_d \eta_d + \beta_d \tilde{\psi}_d, \\ D_{cd} = \chi_d \eta_d + \varrho_d \tilde{\psi}_d, \end{cases} \tag{19}$$

where η_d needs to be at least of dimension $(r - 1 = 1)$ [1,3,11], while the gains $\alpha_d, \beta_d, \chi_d$ and ϱ_d should be designed such that \bar{A} is Hurwitz.

Notice that the tracking error dynamics is formed from the combination of the vector $e_d = [\tilde{\psi}_d \quad \tilde{\eta}_d]^T$ mutually with the compensator state η_d

$$\begin{cases} \dot{E}_d = \bar{A}E_d + \bar{b}[u_{ad} - \delta_d], \\ z_d = \bar{C}E_d, \end{cases} \tag{20}$$

where $E_d = [e_d^T \quad \eta_d^T]^T, \bar{A} = \begin{bmatrix} A - \varrho_d b c & -b \chi_d \\ \beta_d c & \alpha_d \end{bmatrix}, \bar{b} = \begin{bmatrix} b \\ 0 \end{bmatrix}, \bar{c} = \begin{bmatrix} c & 0 \\ 0 & I \end{bmatrix}, A = \begin{bmatrix} 0 & 1 \\ 0 & 0 \end{bmatrix}, b = \begin{bmatrix} 0 \\ 1 \end{bmatrix}, c = \begin{bmatrix} 1 \\ 0 \end{bmatrix}^T$, and z_d is the vector of available measurements.

4.3 Design and analysis of an observer for the error dynamics

A minimal-order observer of dimension $(r - 1 = 1)$ may be designed for the dynamics in (20). However, to streamline the subsequent stability analysis, in what follows, we consider the case of a full-order observer of dimension $(2r - 1 = 3)$ [4,15,21].

To this end, consider the following linear observer for the tracking error dynamics in (20):

$$\begin{cases} \dot{\hat{E}}_d = \bar{A}\hat{E}_d + K(z_d - \hat{z}_d), \\ \hat{z}_d = \bar{C}\hat{E}_d, \end{cases} \tag{21}$$

where K is a gain matrix, and should be chosen such that $\tilde{A} = (\bar{A} - K\bar{C})$ is asymptotically stable. Then, introduce the observer error signal $\tilde{E}_d = (\hat{E}_d - E_d)$ and write the observer error dynamics

$$\begin{cases} \dot{\tilde{E}}_d = \tilde{A}\tilde{E}_d - \bar{b}[u_{ad} - \delta_d], \\ \tilde{z}_d = \bar{C}\tilde{E}_d, \end{cases} \tag{22}$$

where $\tilde{z}_d = (\hat{z}_d - z_d)$.

5 SHL NN Approximation of the Inversion Error

5.1 Neural network approximation

Assume that there exists a neural network with only one single hidden layer that approximates the term of uncertainties δ_d . This NN has an output given by

$$y_i = \sum_{j=1}^{N_2} \left[m_{ij} \Phi \left(\sum_{k=1}^{N_1} n_{jk} x_k + \theta_{nj} \right) + \theta_{mi} \right], \quad x \in \mathfrak{R}^{N_1}, \quad i = 1, \dots, N_3, \quad (23)$$

where $\Phi(\cdot)$ is an activation function, n_{jk} are the first-to-second layer interconnection weights, m_{ij} are the second to third layer interconnection weights, N_2 is associated with the number of neurons in the hidden layer, θ_{nj} and θ_{mi} denote bias terms.

Theorem 5.1 *Given $\epsilon^* > 0$, there exists a set of bounded weights Ψ and N such that the model inversion error $\delta(x, u)$ can be approximated over a compact set $\mathcal{D} \subset \Omega X \mathcal{R}$, by an SHL NN*

$$\delta(\xi_d, v_d) = \Psi^T \Phi(N^T \mu_d) + \epsilon(d, \mu_d), \quad |\epsilon| < \epsilon^*, \quad (24)$$

using the input vector

$$\mu_d(t) = [\nu_d^T(t) \quad \psi_d^T(t)]^T \in \mathcal{D}, \quad \|\mu_d\| \leq \mu_d^*, \quad \mu_d^* > 0. \quad (25)$$

5.2 Adaptive element

The output of an SHL NN defines the adaptive signal

$$u_{ad} = \widehat{\Psi}^T \Phi(N^T \mu_d) + \epsilon(d, \mu_d), \quad (26)$$

where $\widehat{\Psi}$ and \widehat{N} are estimates of Ψ and N that are updated as follows:

$$\begin{aligned} \dot{\widehat{\Psi}} &= -F_d [2(\widehat{\Phi} - \widehat{\Phi}' N^T \mu_d) \widehat{E}_d^T P \bar{b} + k_d (\widehat{\Psi} - \Psi_0)], \\ \dot{\widehat{N}} &= -G_d [2\mu_d \widehat{E}_d^T P \bar{b} \widehat{\Psi}^T \widehat{\Phi}' + k_d (\widehat{N} - N_0)] \end{aligned} \quad (27)$$

in which Ψ_0 is the initial value of Ψ , N_0 is the initial value of the hidden layer weights vector N , $\widehat{\Phi} = \Phi(N^T \mu_d)$, $\widehat{\Phi}'$ denotes the Jacobian matrix, P is the solution of the Lyapunov equation

$$\overline{A}^T P + P \overline{A} = -Q \quad (28)$$

for some $Q > 0$, $k_d > 0$, and F_d, G_d are adaptation gain matrices.

Using (24) and (26), the error dynamics in (20) can be reformulated as

$$\begin{cases} \dot{E}_d = \overline{A} E_d + \bar{b} [\widehat{\Psi}^T \Phi(\widehat{N}^T \mu_d) - \Psi^T \Phi(N^T \mu_d) - \epsilon], \\ z_d = \overline{C} E_d. \end{cases} \quad (29)$$

Define

$$\widetilde{\Psi} = \widehat{\Psi} - \Psi, \quad \widetilde{N} = \widehat{N} - N, \quad Z_d = \begin{bmatrix} \Psi & 0 \\ 0 & N \end{bmatrix}, \quad \widetilde{Z}_d = \begin{bmatrix} \widetilde{\Psi} & 0 \\ 0 & \widetilde{N} \end{bmatrix} \quad (30)$$

and note that $\|\widehat{\Psi}\| < \|\widetilde{\Psi}\| + \Psi^*$, $\|\Psi\| < \Psi^*$, $\|\widehat{N}\|_F < \|\widetilde{N}\|_F + N^*$, $\|N\|_F < N^*$, where Ψ^* and N^* are the upper bounds for the weights in (24), and the subscript F denotes the Frobenius norm. Therefore, the mismatch between the adaptive signal and the inversion errors

$$u_{ad} - \delta_d = \widehat{\Psi}^T \Phi(\widehat{N}^T \mu_d) - \Psi^T \Phi(N^T \mu_d) - \epsilon \tag{31}$$

allows for the following upper bound for some computable α_a, α_b

$$|u_{ad} - \delta_d| \leq \alpha_a \|\widetilde{Z}_d\|_F + \alpha_b, \quad \alpha_a > 0, \quad \alpha_b > 0. \tag{32}$$

Since the weights are adjusted online, we will need the following representation for the stability proof : $\widehat{\Psi}^T \Phi(\widehat{N}^T \mu_d) - \Psi^T \Phi(N^T \mu_d) = \widetilde{\Psi}^T (\widehat{\Phi} - \widehat{\Phi}' \widehat{N}^T \mu_d) + \vartheta_b + \vartheta$, where $\vartheta = \widetilde{\Psi}^T \widehat{\Phi}' N^T \mu_d - \Psi^T \mathcal{O}(\widetilde{N}^T \mu_d)^2$, and $\vartheta_b = \widetilde{\Psi}^T \widehat{\Phi}' \widetilde{N}^T \mu_d$.

Such a representation is achieved via the Taylor series expansion of $\Phi(N^T \mu_d)$ around the estimates $\widehat{N}^T \mu_d$. Taking account of the bound in (25), a bound for $(\vartheta - \epsilon)$ over a compact can be expressed as follows [1, 4, 15]

$$|\vartheta - \epsilon| \leq \gamma_a \|\widetilde{Z}_d\|_F + \gamma_b, \quad \gamma_a > 0, \gamma_b > 0, \tag{33}$$

where γ_a and γ_b are computable constants, γ_a depends upon unknown constant μ_d^* , and γ_b upon ϵ^* . Thus, the forcing term in (17) can be written

$$u_{ad} - \delta_d = \widetilde{\Psi}^T (\widehat{\Phi} - \widehat{\Phi}' \widehat{N}^T \mu_d) + \widehat{\Psi}^T \widehat{\Phi}' \widetilde{N}^T \mu_d + \vartheta - \epsilon. \tag{34}$$

6 Stability Analysis

We confirm through Lyapunov’s direct method that if the initial errors of the variables $E_d^T, \widetilde{E}_d^T, \widetilde{\Psi}$ and \widetilde{N} belong to the presented compact set, then the composite error vector $\zeta_d = [E_d^T \quad \widetilde{E}_d^T \quad \widetilde{Z}_d^T]^T$ is ultimately bounded. Notice that ζ_d can be viewed as a function of the state variables $\xi_d, \eta_d, \widetilde{E}_d, \widetilde{Z}_d$, the command vector $y_c = [\psi_d^* \quad \psi_d^{*}]^T$, and a constant vector Z_d

$$\zeta_d = F(\xi_d, \eta_d, \widehat{E}_d, \widehat{Z}_d, y_c, Z_d). \tag{35}$$

The relation in(35) represents a mapping from the original domains of the arguments to the space of the error variables

$$F : \Omega_{\xi_d} \times \Omega_{y_c} \times \Omega_{\eta_d} \times \Omega_{\widehat{E}_d} \times \Omega_{\widehat{Z}_d} \times \Omega_{Z_d} \longrightarrow \Omega_{\zeta_d}. \tag{36}$$

Recall that (25) introduces the compact set \mathcal{D} over which the NN approximation is valid. From (25), it follows that

$$\mu_d \in \mathcal{D} \iff \xi_d \in \Omega_{\xi_d}, \quad v_d \in \Omega_{v_d}. \tag{37}$$

Also, notice that, since the observer in(21) is driven by the output tracking error $\widetilde{\psi}_d = \psi_d^* - \psi_d$ and compensator state η_d , having $\xi_d \in \Omega_{\xi_d}$, $y_c \in \Omega_{y_c}$, $\eta_d \in \Omega_{\eta_d}$ implies that $\widehat{E}_d \in \Omega_{\widehat{E}_d}$, the latter being a compact set.

According to (13)

$$v_d = F_{v_d}(\eta_d, \widehat{E}_d, \widehat{Z}_d, y_c), \tag{38}$$

where $F_{v_d} : \Omega_{\eta_d} \times \Omega_{\widehat{E}_d} \times \Omega_{\widehat{Z}_d} \times \Omega_{y_c} \longrightarrow \Omega_{v_d}$. Thus, (38), (37) and (35) ensure that Ω_{ζ_d} is a bound set. Introduce the largest ball, which is included in Ω_{ζ_d} in the error space

$$B_R = \{|\zeta_d| \leq R\}, \quad R > 0. \tag{39}$$

For every $\zeta_d \in B_R$, we have $\mu_d \in \mathcal{D}$, $Z_d \in \Omega_{Z_d}$, where both \mathcal{D} and Ω_{Z_d} are bounded sets.

Assumption 6.1 Assume

$$R > \gamma \sqrt{\frac{T_M}{T_m}} \geq \gamma, \quad (40)$$

where T_M and T_m are the maximum and minimum eigenvalues of the following matrix

$$T = \begin{bmatrix} 2P & 0 & 0 & 0 \\ 0 & 2\tilde{P} & 0 & 0 \\ 0 & 0 & F_d^{-1} & 0 \\ 0 & 0 & 0 & G_d^{-1} \end{bmatrix} \quad (41)$$

and

$$\Upsilon = \max\left(\sqrt{\frac{\|P\bar{b}\|^2\gamma_b^2+k_2^2+\bar{Z}_d}{\lambda_{\min}(Q)-2}}, \sqrt{\frac{\|P\bar{b}\|^2\gamma_b^2+k_2^2+\bar{Z}_d}{\lambda_{\min}(\tilde{Q})-2}}, \sqrt{\frac{\|P\bar{b}\|^2\gamma_b^2+k_2^2+\bar{Z}_d}{\frac{k_d}{2}-k_1^2-[\gamma_a\|P\bar{b}\|]^2}}\right), \text{ where } \bar{Z}_d = \frac{k_d}{2} \left[\|\Psi - \Psi_0\| \right]^2, k_d > 2 \left[k_1^2 + \gamma_a^2 \|P\bar{b}\|^2 \right], k_1 = \Theta\alpha_a + \|P\bar{b}\|\gamma_a, k_2 = \Theta\alpha_b + \|P\bar{b}\|\gamma_b, \Theta = \|P\bar{b}\| + \|\tilde{P}\bar{b}\| \text{ and } \tilde{P} \text{ satisfies } \tilde{A}^T \tilde{P} + \tilde{P} \tilde{A} = -\tilde{Q} \text{ for some } \tilde{Q} > 0 \text{ with minimum eigenvalues } \lambda_{\min}(\tilde{Q}) > 2.$$

Theorem 6.1 Let the assumption (6.1) hold, and let $\lambda_{\min}(Q) > 2$ for Q introduced in (28). Then, if the initial errors belong to the compact set Ω_α , defined in (43), the feedback control law given by (5) and (13), along with (27), guarantees that the signals $E_d, \tilde{E}_d, \tilde{N}$ and $\tilde{\Psi}$ in the closed-loop system are ultimately bounded.

Proof. Consider the following Lyapunov function for the system in (22) and (29):

$$V = E_d^T P E_d + \tilde{E}_d^T \tilde{P} \tilde{E}_d + \frac{1}{2} \tilde{\Psi}^T F_d^{-1} \tilde{\Psi} + \frac{1}{2} \text{tr}(\tilde{N}^T G_d^{-1} \tilde{N}). \quad (42)$$

The derivative of V along (22), (29), (34), and with the definition of $\tilde{E}_d = \hat{E}_d - E_d$, can be written as

$$\begin{aligned} \dot{V} = & -E_d^T P E_d - \tilde{E}_d^T \tilde{Q} \tilde{E}_d + 2\hat{E}_d^T P \bar{b} [\vartheta - \epsilon] - 2\tilde{E}_d^T (\tilde{P} \bar{b} + P \bar{b}) [u_{ad} - \delta_d] \\ & - k_d \tilde{\Psi}^T (\tilde{\Psi} - \Psi_0) - k_d \text{tr}[\tilde{N}^T (\hat{N} - N_0)]. \end{aligned}$$

Using upper bounds from (32) and (33), the following property for vectors $\text{tr}[\tilde{N}^T (\hat{N} - N_0)] = \frac{1}{2} \|\tilde{N}\|_F^2 + \frac{1}{2} \|\hat{N} - N_0\|_F^2 - \frac{1}{2} \|N - N_0\|_F^2$, and completing squares twice, the upper bound reduces to [15]

$$\begin{aligned} \dot{V} \leq & -(\lambda_{\min}(Q) - 2) \|E_d\|^2 + 2\gamma_b^2 \|P\bar{b}\|^2 - (\lambda_{\min}(\tilde{Q}) - 2) \|\tilde{E}_d\|^2 + k_2^2 \\ & - \left(\frac{k_d}{2} - k_1^2 - [\gamma_a \|P\bar{b}\|]^2 \right) \|\tilde{Z}_d\|_F^2 + \bar{Z}_d. \end{aligned}$$

Either of the following conditions:

$$\|E_d\| > \sqrt{\frac{\|P\bar{b}\|^2\gamma_b^2+k_2^2+\bar{Z}_d}{\lambda_{\min}(Q)-2}}, \|\tilde{E}_d\| > \sqrt{\frac{\|P\bar{b}\|^2\gamma_b^2+k_2^2+\bar{Z}_d}{\lambda_{\min}(\tilde{Q})-2}}, \|\tilde{Z}_d\|_F > \sqrt{\frac{\|P\bar{b}\|^2\gamma_b^2+k_2^2+\bar{Z}_d}{\frac{k_d}{2}-k_1^2-[\gamma_a\|P\bar{b}\|]^2}}$$

will render $\dot{V} < 0$ outside a compact set: $B_\Upsilon = \{\zeta_d \in B_R, \|\zeta_d\| \leq \Upsilon\}$.

Note from (40) that $B_\Upsilon \subset B_R$. Then, consider the Lyapunov function candidate in (42) and write it as $V = \zeta_d^T T \zeta_d$. Let Γ be the maximum value of the Lyapunov function V on the edge of B_Υ : $\Gamma = \max_{\|\zeta_d\|=\Upsilon} V = \Upsilon^2 T_M$.

Introduce the level set $\Omega_\Upsilon = \{\zeta_d, V = \Gamma\}$. Let α_v be the minimum value of the Lyapunov function V on the edge of B_R : $\alpha_v = \min_{\|\zeta_d\|=R} V = R^2 T_m$. Define the level set

$$\Omega_\alpha = \{\zeta_d \in B_R, V = \alpha_v\}. \quad (43)$$

The condition in (40) ensures that $\Omega_\Upsilon \subset \Omega_\alpha$, and thus ultimate boundedness of ζ_d .

7 Simulation Results

In this section, computer simulations inquire the performances of the proposed control scheme in the presence of structured and unstructured uncertainties. The physical and electrical parameters of the two-phase IM under investigation are: $L_m = 0.0117H$, $R_r = 3.9\Omega$, $R_s = 1.7\Omega$, $L_r = 0.014H$, $L_s = 0.014H$, $f = 0.00014N.m/rad/sec$ and $J = 0.00011kg.m^2$ [12].

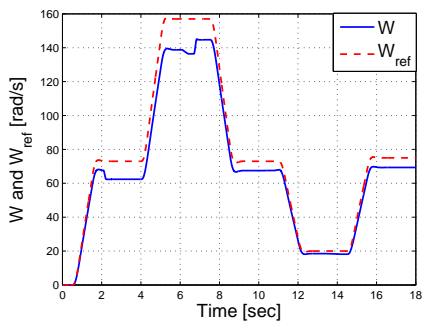
One has chosen the design parameters for the dynamic compensators as follows: $\alpha_d = -85$, $\beta_d = 10$, $\chi_d = -18005$ and $\varrho_d = 2376$, $\alpha_q = -105$, $\beta_q = 1$, $\chi_q = -324090$ and $\varrho_q = 3376$ in order to place the poles of both closed-loop error dynamics at $(-35, -25 \mp j)$ and $(-15, -45 \mp j)$, respectively (refer to [1,3] for more details). The observer dynamics in (29) was designed so that its poles are five times faster than those of the error dynamics. We implement ten neurons in the hidden layer of the neural network that approximate δ_d , while we employ eight neurons in the hidden layer of the NN that approximate δ_q . For the neural network, we use the following sigmoidal basis function $\Phi(x) = \frac{1}{1+e^{-ax}}$ with $a = 1$. The adaptation gains were set to $F_d = G_d = 2I$, with sigma modification gains $k_d = 0.365$.

7.1 Test of robustness of the adaptive control

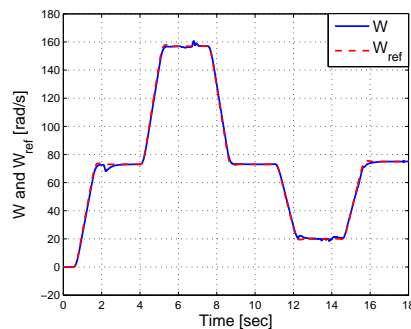
To demonstrate that the proposed approach is successfully applicable for the nonlinear IM system in the presence of high uncertainties, the rate of (δ) will be varied with ($\pm 50\%$ then $\pm 100\%$) of its norm value. Once again, our perspective is to develop an adaptive controller for each subsystem of the decoupled dynamics of the IM using only one SHL NN, in which the adaptive terms (u_{ad} and u_{aq}) overcome the effects of inversion errors (δ_d and δ_q), what bring to force the system measurements (ψ_d) and (w) to track reference trajectories (ψ_d^*) and (w^*), respectively, with bounded errors.

The simulation results depicted in Figures 2 illustrate the performance comparison of the considered control systems for the case (δ is varied) without and with NN. In these figures, we illustrate clearly that the adaptive control augmented via only SHL NN works well, and excellent tracking accuracy is obtained. To explain, the tracking of the speed signal to its reference is close enough so that they are indistinguishable in Figure 2(b), which proves that the NN augmentation (u_{aq}) identifies successfully the inversion error (δ_q), as illustrated in Figure 3(a). Furthermore, Figure 2(d) reports that the flux response is compatible with respect the imposed flux reference trajectory. This is due essentially to the ability of a the SHL NN (u_{ad}) to model nonlinearities (δ_d) on-line, as presented in Figure 3(b). Moreover, from Figures 3(c) and 3(d) it is worth noticing that the proposed approach has achieved excellent responses both at transient and steady state process.

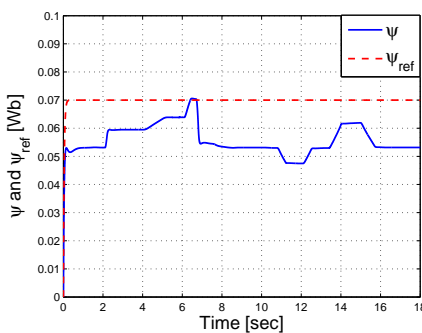
The proposed control system is able to achieve flux and speed tracking high accuracy with an admissible regulation performance with respect to load disturbances and adequate robustness against parameter variations.



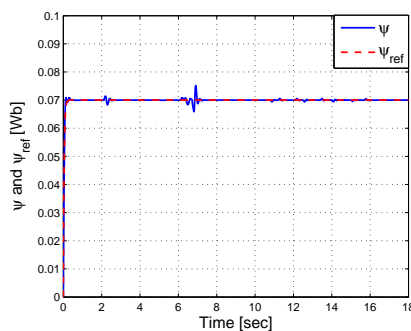
(a) W and W^* without NN.



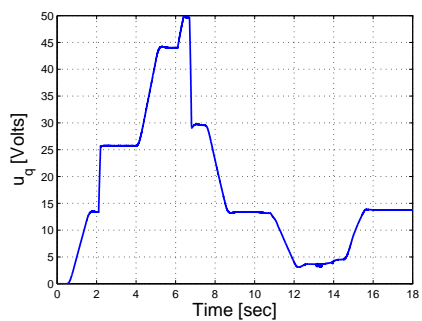
(b) W and W^* with SHL NN.



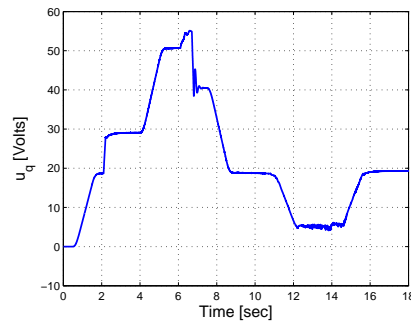
(c) ψ_d and ψ_d^* without NN.



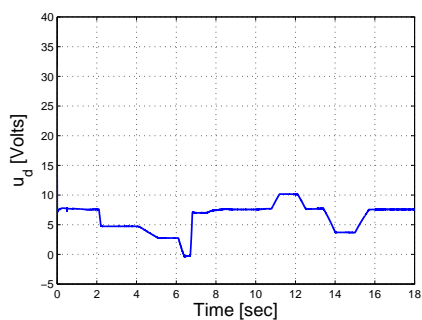
(d) ψ_d and ψ_d^* with SHL NN.



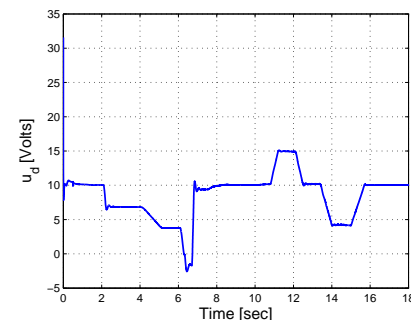
(e) u_q without NN.



(f) u_q with SHL NN.



(g) u_d without NN.



(h) u_d with SHLNN.

Figure 2: Simulation results with variation of uncertainties: without NN ((a), (c), (e), (g)), and with NN ((b), (d), (f), (h)).

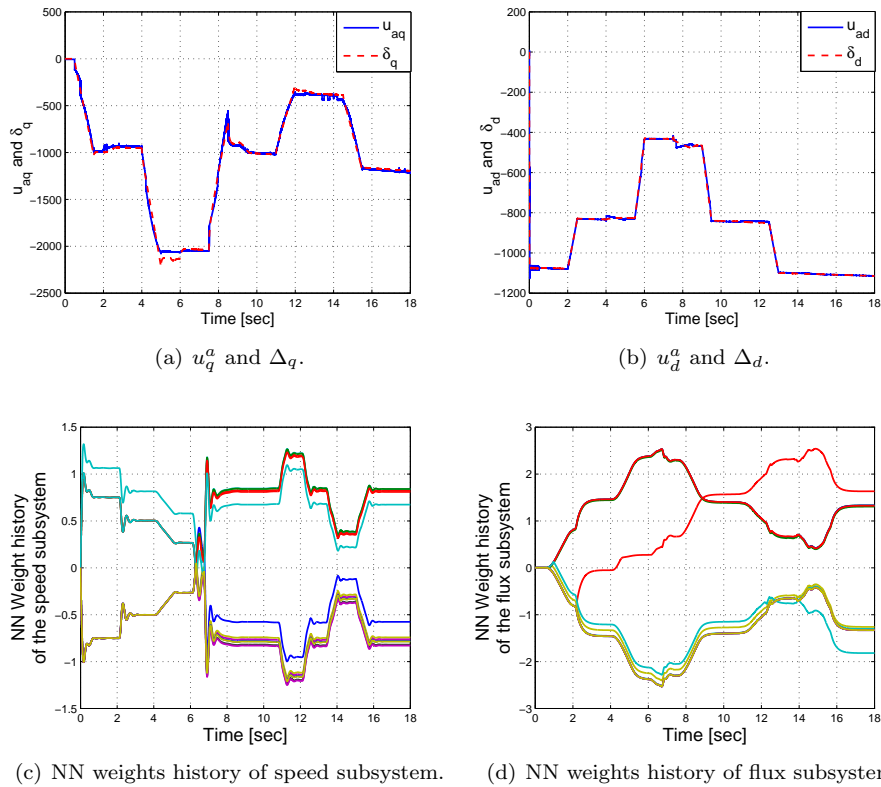


Figure 3: ((a), (b)) Identification of uncertainties (δ) by NN. ((c), (d)) NN weight history.

8 Summary

The fundamental goal of this paper consisted in realizing a tracking accuracy for multi-inputs multi-outputs nonlinear induction motor in the presence of high uncertainties. First, an appropriate input-output feedback linearizing controller is applied to decouple the speed dynamics from the flux. Then, the nonlinear state feedback controller is involved as a linearizing control. After, the adaptive control augmented via only nonlinearly parameterized SHL NNs is introduced to cancel the uncertainties existing in the induction motor. A linear observer is introduced to estimate the derivatives of the tracking errors. These estimates are used as inputs to the NN and in the adaptation laws as an error signal. Of particular interest, ultimate boundedness of error signals is shown using Lyapunov’s direct method. Finally, computer simulations are undertaken to highlight the effectiveness of the proposed adaptive controller. As a future research we will propose to add other NN structures for sensorless control.

References

- [1] H. Ait Abbas, M. Belkheiri and Z. Boubakeur. Feedback Linearization Control for Highly Uncertain Nonlinear Systems Augmented by Single- Hidden-Layer Neural Networks. *Jour-*

- nal of Engineering Science and Technology Review* **8** (2) (2015) 215–224.
- [2] H. A. Abbas, B. Zegnini, and M. Belkheiri. Neural network-based adaptive control for induction motors. In: *The 12th IEEE International Multi-Conference on Systems, Signals and Devices*, (DOI:10.1109/SSD.2015.7348180), (16-19 March 2015), Mahdia-Tunisia.
 - [3] H. A. Abbas, B. Zegnini, M. Belkheiri, and A. Rabhi. Radial basis function neural network-based adaptive control of uncertain nonlinear systems. In: *Control, Engineering and Information Technology (CEIT)*, 2015, 3rd International Conference on IEEE, (2015), 1–6.
 - [4] H. Ait Abbas, M. Belkheiri, and B. Zegnini. Robust Neural Output Feedback Tracking Control For a Class of Uncertain Nonlinear Systems Without Time-delay. *Nonlinear Dynamics and Systems Theory* **16** (2) (2016) 115–128.
 - [5] H. Ait Abbas, M. Belkheiri, and B. Zegnini. Feedback Linearization Control of an Induction Machine Augmented by Single Hidden Layer Neural Networks. *International Journal of Control*, (DOI. 10.1080/00207179.2015.1063162), **89** (1) (2016) 140–155.
 - [6] E. Arbin and M. Gregory. Adaptive Backstepping Control of a Speed-Sensorless Induction Motor Under Time-Varying Load Torque and Rotor Resistance Uncertainty. In: *Proc. of the 38th Southeastern Symposium on System Theory*, (March 5-7, 2006), 512–518, USA.
 - [7] M. Belkheiri and F. Boudjema. Neural network augmented backstepping control for an induction machine. *International Journal of Modelling, Identification and Control* **5** (4) (2008) 288–296.
 - [8] M. Belkheiri, H. Ait Abbas, & B. Zegnini. Feedback Linearization Control of Non-linear Uncertain Systems Using Single Hidden Layer Neural Networks. In: *The 11th IEEE International Multi-Conference on Systems, Signals and Devices*, (DOI: 10.1109/SSD.2014.6808779), (February 11–14, 2014), Castelldefels-Barcelona, Spain.
 - [9] M. Benrejeb, M. Gasmi, and P. Borne. New stability conditions for TS fuzzy continuous nonlinear models. *Nonlinear Dynamics and Systems Theory* **5** (4) (2005) 369–379.
 - [10] N. Bounar, A. Boulkroune, F. Boudjema, M. M'Saad, M. Farza. Adaptive fuzzy vector control for a doubly-fed induction motor. *Neurocomputing* **151** (2) (2014) 756–769.
 - [11] J. Brasch, & J. Pearson. Pole placement using dynamic compensators. *IEEE Trans. Automat. Contr.* **AC-15** (Jan. 1970) 34–43.
 - [12] J. Chiasson. *Modeling and High Performance Control of Electric Machines*. John Wiley & Sons, New Jersey, 2005.
 - [13] L. Chuan-Kai. RBF neural network-based adaptive critic control of induction motors. *Applied Soft Computing* **11** (3) (2011) 3066–3074.
 - [14] N. Henini, L. Nezli, A. Tlemani and M. O. Mahmoudi. Improved Multimachine Multiphase Electric Vehicle Drive System Based on New SVPWM Strategy and Sliding Mode – Direct Torque Control. *Nonlinear Dynamics and Systems Theory* **11** (4) (2011) 425–438.
 - [15] N. Hovakimyan, F. Nardi, A. Calise and N. Kim, Adaptive Output Feedback Control of Uncertain Nonlinear Systems Using Single-Hidden-Layer NNs. *IEEE Trans. on Neural Networks* **13** (6) (2002) 1420–1431.
 - [16] Y. Jeon, B. Chen and H. Yu. Position tracking control of induction motors via adaptive fuzzy backstepping. *Energy Conversion and Management* **51** (11) (2010) 2345–2352.
 - [17] J. Zhou, C. Wen, and Y. Zhang. Adaptive Output Control of a Class of Time-Varying Uncertain Nonlinear Systems. *Nonlinear Dynamics and Systems Theory* **5** (3) (2005) 285–298.
 - [18] Z. Kardous and N. B. Braiek. Stabilizing Sliding Mode Control for Homogeneous Bilinear Systems. *Nonlinear Dynamics and Systems Theory* **14** (3) (2014) 303–312.

- [19] S. Melliani, A. El Allaoui, and L. S. Chadli. Relation Between Fuzzy Semigroups and Fuzzy Dynamical Systems. *Nonlinear Dynamics and Systems Theory* **17** (1) (2017) 60–69.
- [20] F. Nardi, F., & A. J. Calise. Robust adaptive nonlinear control using single hidden layer neural networks. In: *Proc. Conf. Decision Contr.* **4** (2000) 3825–3830.
- [21] S. Xu, P. Shi, C. Feng, Y. Guo, and Y. Zou. Robust Observers for a Class of Uncertain Nonlinear Stochastic Systems with State Delays. *Nonlinear Dynamics and Systems Theory* **4** (3) (2004) 369–380.